

Wheel-Axle Topology Driven Halogen Bonds: Formation of Ladder, 1D and 2D Networks in Hexa-coordinated Sn(IV)Porphyrins

Jyoti Rani,^a Gurkiran Kaur,^a Sushila,^a Diksha,^a Rashmi Yadav,^a Ramesh Kataria,^a Venugopalan Paloth,^a Palani Natarajan,^a Arvind Chaudhary^b and Ranjan Patra^{*a}

^a*Department of Chemistry and Centre for Advanced Studies in Chemistry, Panjab University, Chandigarh-160014, India.*

^b*Science and Engineering Research Board, New Delhi-110070, India.*

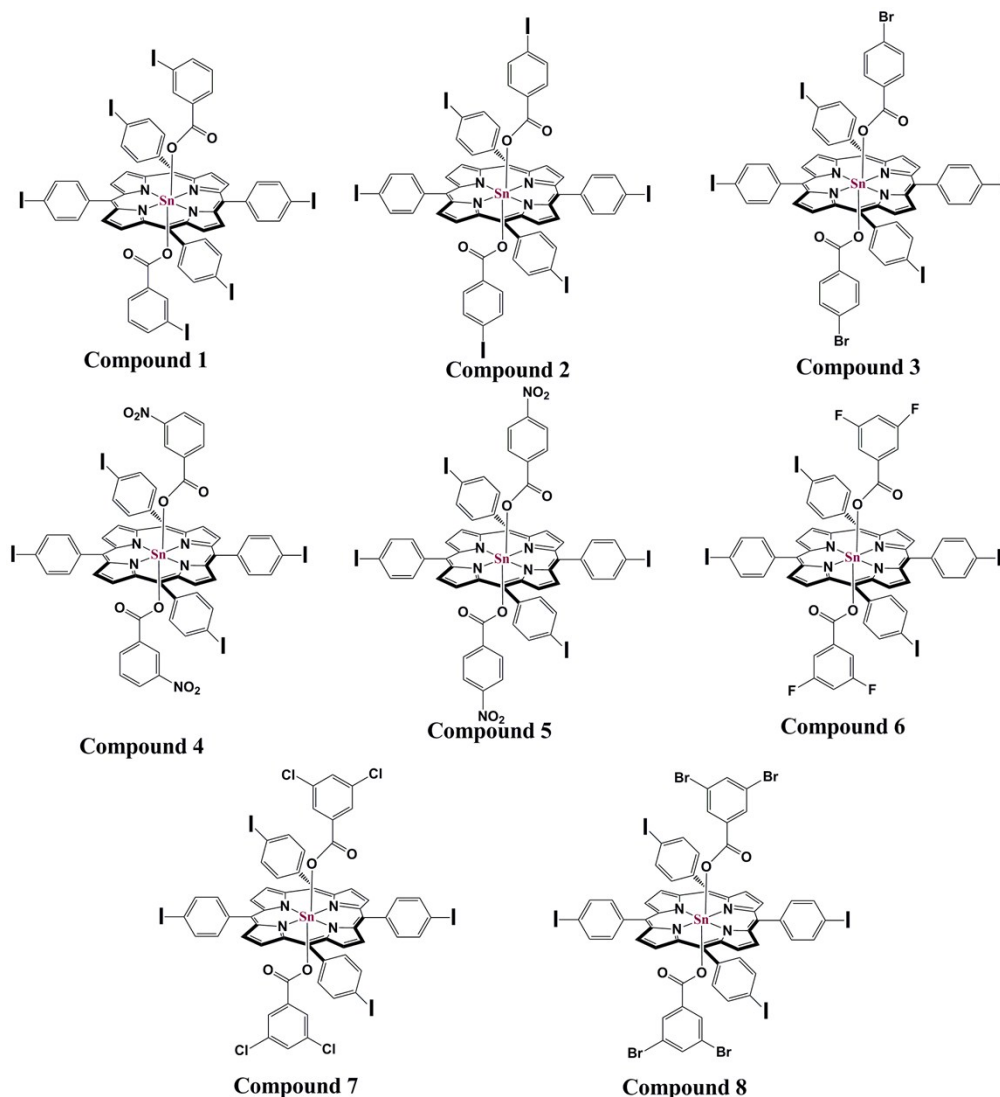
Email: ranjanpatra06@gmail.com

EXPERIMENTAL SECTION

Materials: Pyrrole, 4-iodobenzaldehyde, 3-iodobenzoic acid, 4-iodobenzoic acid, 4-bromobenzoic acid, 3-nitrobenzoic acid, 4-nitrobenzoic acid, 3,5-fluorobenzoic acid, 3,5-chlorobenzoic acid, 3,5-bromobenzoic acid were obtained from TCI chemicals. Solvents like propionic acid, chloroform, dimethylformamide (DMF), diethyl ether and hexane were obtained commercial sources and purified by standard procedures before use. Free-base porphyrins were prepared following the Adler method.¹ Sn(TIPP)(OH)₂ were prepared by literature methods.²

Physical Measurements.

UV-Vis spectra were recorded on a Perkin Elmer UV-Vis-NIR spectrometer. IR spectra were recorded on a Bruker Tensor 27 system spectrophotometer in ATR mode.



Scheme S1: Schematic illustration of the Sn(IV)-5,10,15,20-*meso*-tetrakis(4-iodophenyl)porphyrin scaffolds used in this study. Axial ligands (L) 3-Iodo benzoic acid (**1**), 4-Iodo benzoic acid (**2**), 4-Bromo benzoic acid (**3**), 3-Nitro benzoic acid (**4**), 4-Nitro benzoic acid (**5**), 3,5-difluoro benzoic acid (**6**), 3,5-dichloro benzoic acid (**7**), 3,5-dibromo benzoic acid (**8**).

General procedure of synthesis of the complexes:

A mixture of trans-Dihydroxo[5,10,15,20-tetrakis(4-iodophenyl)porphyrinato]tin(IV) (0.01 mmol) was dissolved in 5 ml of CHCl_3 and corresponding halogenated/nitro functionalized phenyl carboxylic acid (0.025 mmol) was dissolved in 0.5 mL of DMF. The resulting solution was heated for 1 h at 70 °C in a bath reactor. After cooling, the mixture was left for slow evaporation at ambient conditions; a dark purple solid was precipitated out. Filter the solid and wash with hexane. All the complexes were isolated in more than 60% yield.

Compound 1. X-ray quality crystals were obtained by slow evaporation of DMF-CHCl₃ (1:10) solution of **1** into the diethyl ether. After 7 days fine pink crystal of complex were obtained. Yield (7.9 mg, 78%). FT-IR (KBr, cm⁻¹) 2929, 1658, 1462, 1259, 1058, 798, 755, 673, 526, 460. UV-Vis in DCM: λ_{max}/nm (log e) 425(5.48), 556(2.98), 596(2.15).

Compound 2. X-ray quality crystals were obtained diffusion of DMF-CHCl₃ (1:10) solution of compound **2** into the hexane. After 7 days fine pink crystal of complex were obtained. Yield (7.9 mg, 78%). FT-IR (KBr, cm⁻¹) 2917, 1662, 1462, 1213, 1030, 797, 758, 673, 562, 457. UV-Vis in DCM: λ_{max}/nm (log e) 426(5.46), 558(2.92), 598(2.12).

Compound 3. X-ray quality crystals were obtained slow diffusion of CHCl₃ solution of compound **3** into the diethyl ether. After 10 days fine pink crystal of complex were obtained. Yield (7.9 mg, 78%). FT-IR (KBr, cm⁻¹) 1662, 1466, 1213, 1036, 798, 758, 673, 562, 457. UV-Vis in DCM: λ_{max}/nm (log e) 426(5.48), 556(2.88), 595(2.18).

Compound 4. X-ray quality crystals were obtained slow evaporation of CHCl₃ solution of compound **4** into cyclohexane. After 8-9 days fine pink crystal of complex were obtained. Yield (7.9 mg, 78%). FT-IR (KBr, cm⁻¹) 2921, 1674, 1466, 1211, 1059, 804, 712, 650, 567, 459. UV-Vis in DCM: λ_{max}/nm (log e) 425(5.48), 555(2.98), 595(2.15).

Compound 5. X-ray quality crystals were obtained slow evaporation of CHCl₃ solution of compound **5**. After 7-8 days fine pink crystal of complex were obtained. Yield (7.9 mg, 78%). FT-IR (KBr, cm⁻¹) 1707, 1442, 1207, 1031, 785, 761, 660, 575, 449. UV-Vis in DCM: λ_{max}/nm (log e) 425(5.48), 556(2.98), 596(2.15).

Compound 6. X-ray quality crystals were obtained slow evaporation of CHCl₃ and 0.5 DMSO mixture (in place of DMF) of compound **6** into diethyl ether. After 8-10 days fine pink crystal of complex were obtained. Yield (7.9 mg, 78%). FT-IR (KBr, cm⁻¹) 2929, 1646, 1474, 1211, 1030, 804, 759, 659, 562, 459. UV-Vis in DCM: λ_{max}/nm (log e) 425(5.48), 556(2.98), 596(2.15).

Compound 7. X-ray quality crystals were obtained slow evaporation of DMF-CHCl₃ (1:10) solution of compound **7** into diethyl ether. After 10-12 days fine pink crystal of complex were obtained. Yield (7.9 mg, 78%). FT-IR (KBr, cm⁻¹) 3080, 1651, 1466, 1208, 1053, 797, 777, 663, 583, 437. UV-Vis in DCM: λ_{max}/nm (log e) 425(5.48), 556(2.98), 596(2.15).

Compound 8. X-ray quality crystals were obtained slow evaporation of CHCl_3 solution of compound **8** into diethyl ether. After 8-9 days fine pink crystal of complex were obtained. Yield (7.9 mg, 78%). FT-IR (KBr, cm^{-1}) 2917, 1646, 1470, 1217, 1061, 804, 736, 665, 564, 432. UV-Vis in DCM: $\lambda_{\text{max}}/\text{nm}$ (log ϵ) 425(5.48), 556(2.98), 596(2.15).

Crystal Structure Determinations. Single-crystal X-ray diffraction data for compound **1-8** were collected with ‘SuperNova Diffractometer’ equipped with HyPix3000 detector from Rigaku Oxford Diffraction at 293K. Data collection and reduction were performed with inbuilt program suite (CrysAlisPro 1.171.39.33c (Rigaku OD, 2017)) and an absorption correction (multi-scan method) was also done. Structures were solved by the direct method using SHELXS-97 and was refined on F^2 by full-matrix least-squares technique using the SHELXL-2018/3³ program package on WINGX⁴ platform. All non hydrogen atoms were refined anisotropically. Hydrogen atoms were fixed at their stereo-chemical positions and were riding with their respective non-hydrogen atoms with SHELXL default parameters. Compound **5** and **6** have disorder solvent molecule present in the crystal lattice. Disorder CHCl_3 and DMSO molecule was refined isotropically. Complete details of data collection and refinement parameters are recorded in Table-1 in main manuscript.

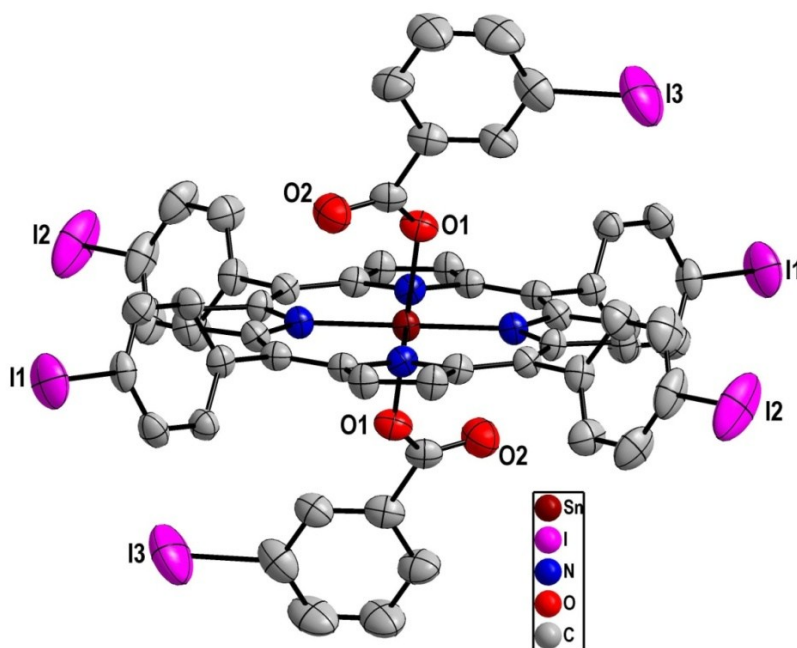


Figure S1. Perspective view of compound **1** showing 45% thermal ellipsoids for all non-hydrogen atoms at 293 K (H-atoms have been omitted for clarity).

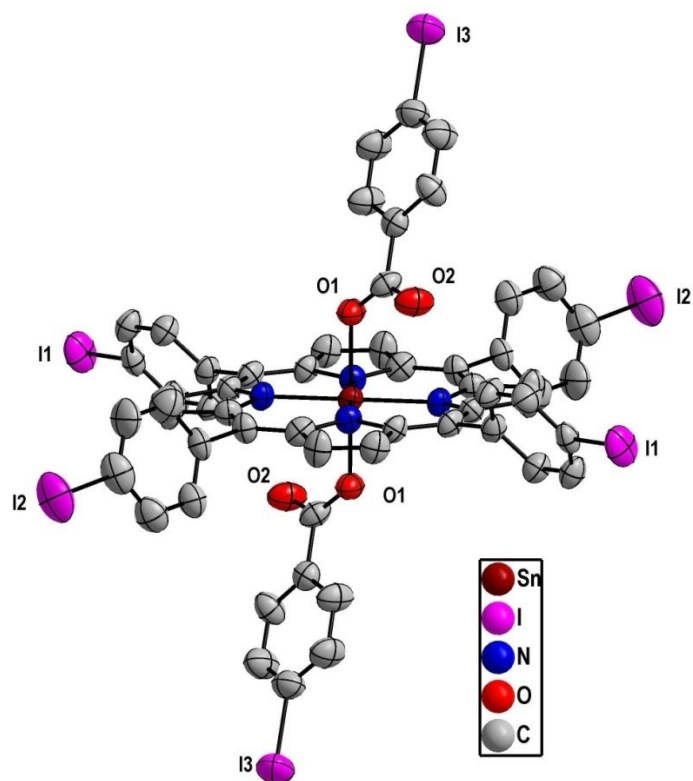


Figure S2. Perspective view of compound **2** showing 45% thermal ellipsoids for all non-hydrogen atoms at 293 K (H-atoms have been omitted for clarity).

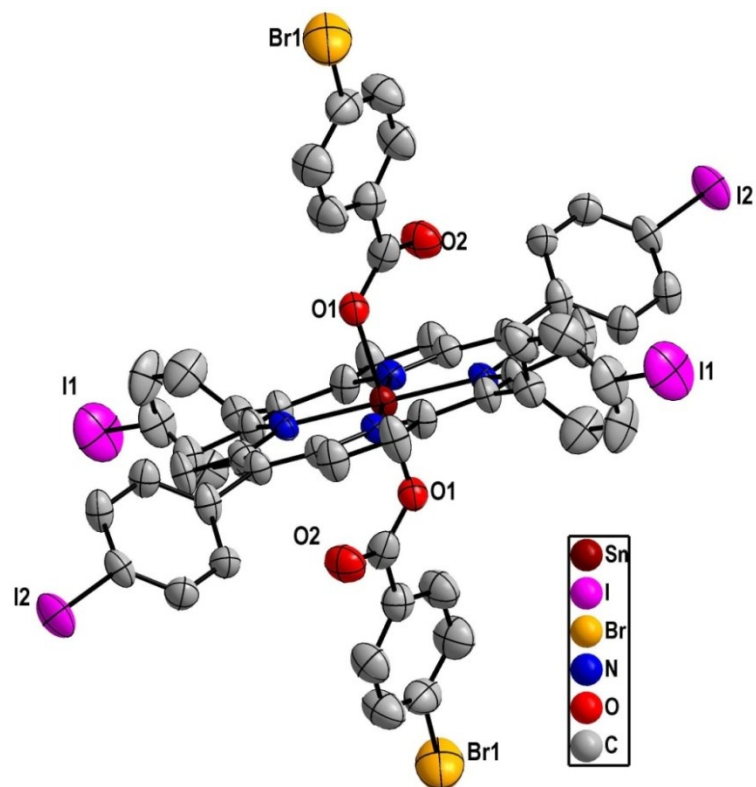


Figure S3. Perspective view of compound **3** showing 45% thermal ellipsoids for all non-hydrogen atoms at 293 K (H-atoms have been omitted for clarity).

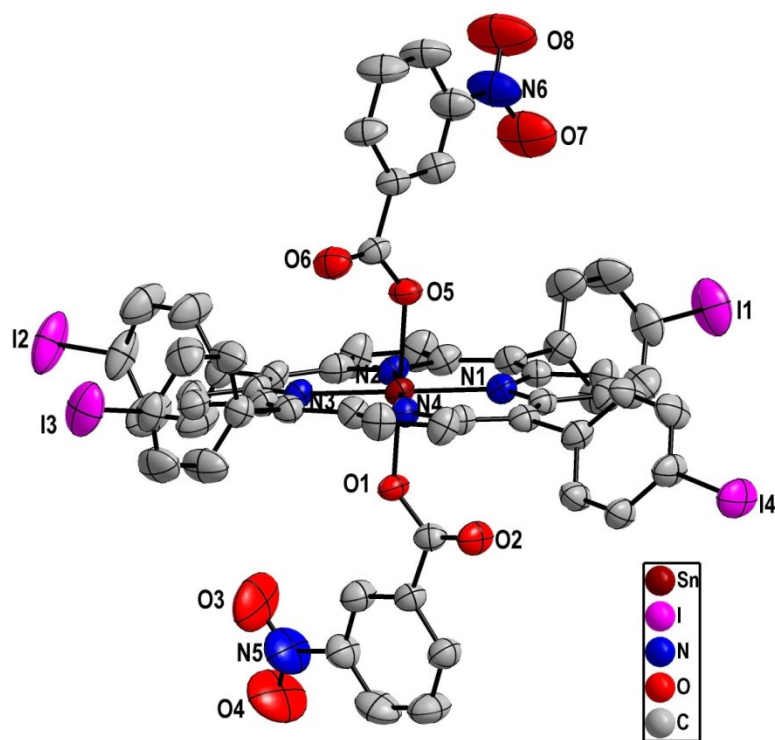


Figure S4. Perspective view of compound **4** showing 35% thermal ellipsoids for all non-hydrogen atoms at 293 K (H-atoms have been omitted for clarity).

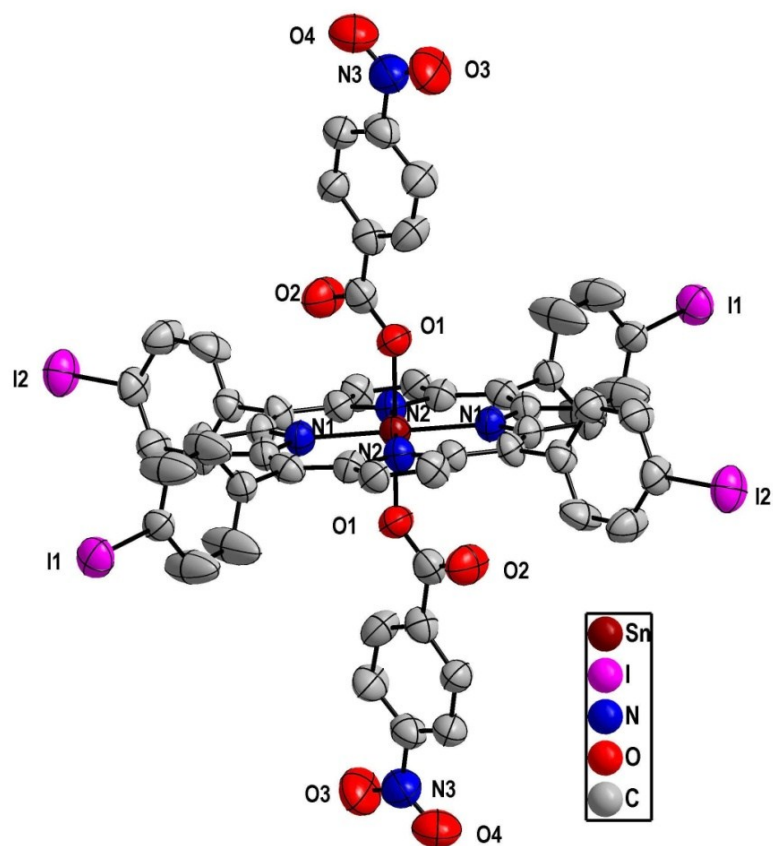


Figure S5. Perspective view of compound **5** showing 45% thermal ellipsoids for all non-hydrogen atoms at 293 K (H-atoms have been omitted for clarity).

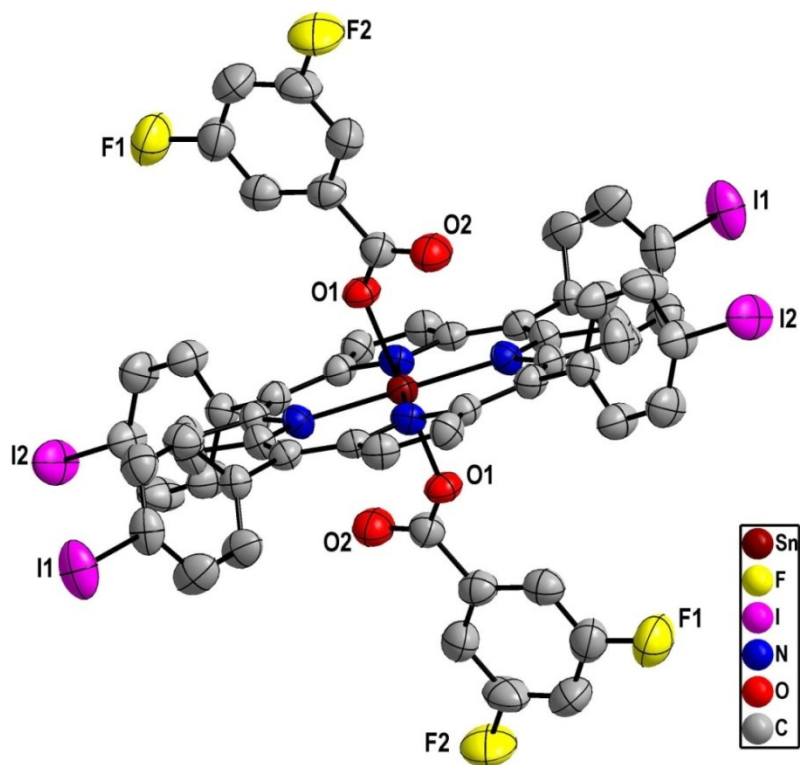


Figure S6. Perspective view of compound 6 showing 45% thermal ellipsoids for all non-hydrogen atoms at 293 K (H-atoms have been omitted for clarity).

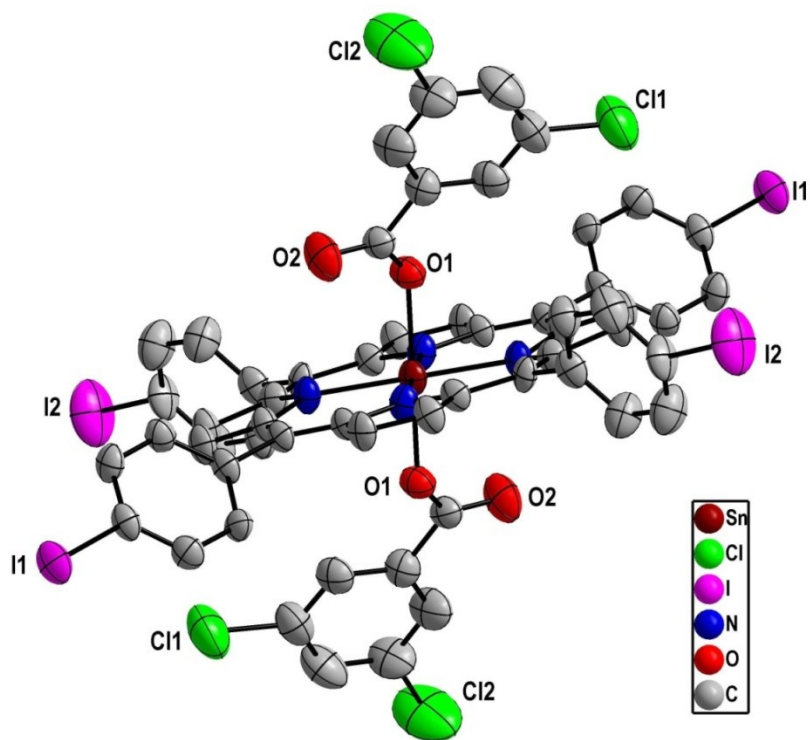


Figure S7. Perspective view of compound **7** showing 45% thermal ellipsoids for all non-hydrogen atoms at 293 K (H-atoms have been omitted for clarity).

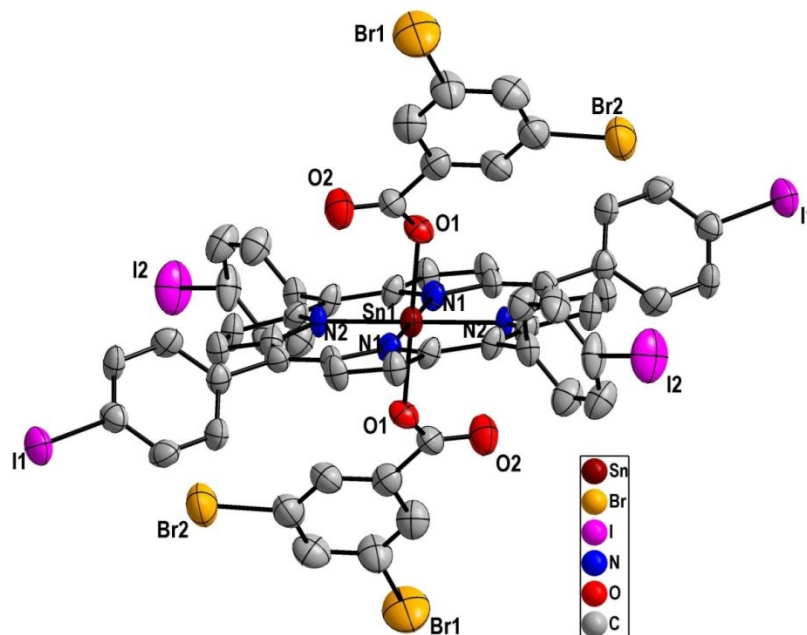


Figure S8. Perspective view of compound **8** showing 45% thermal ellipsoids for all non-hydrogen atoms at 293 K (H-atoms have been omitted for clarity).

Computational Details:

DFT calculations have been carried out by employing a B3LYP hybrid functional using Gaussian 09, revision B.05, package.⁵ Using the method of Becke's three-parameter hybrid exchange functional,⁶ the nonlocal correlation provided by the Lee, Yang, and Parr expression,⁷ and Vosko, Wilk, and Nussair 1980 correlation functional (III) for local correction. The basis set was LANL2DZ for the Sn and I-atom and 6-31G** for C, N, O, Br and H-atom. The coordinates are taken directly from the single-crystal X-ray data. Geometry optimization of compound **2** and **8** was performed. Molecular electrostatic potential surfaces were calculated from optimized geometry.

References:

1. Adler, A. D.; Longo, F. R.; Finarelli, J. D.; Goldmacher, J.; Assour, J.; Korsakoff, L. *J. Org. Chem.* **1967**, *32*, 476.
2. Patra, R.; Titi, H. M.; Goldberg, I. *Cryst. Growth Des.* **2013**, *13*, 1342.

3. Sheldrick GM. SHELXS version-**2018/3** and SHELXL version-**2018/3**: programs for crystal structure solution and refinement. University of Gottingen, Germany, **2018**.
4. L. J. Farrugia, *J. Appl. Crystallogr.*, **1999**, 32, 837-838.
5. Gaussian 09, Revision A.1, Frisch, M. J.; Trucks, G. W.; Schlegel, H. B.; Scuseria, G. E.; Robb, M. A. ; Cheeseman, J. R.; Scalmani, G.; Barone, V.; Mennucci, B.; Petersson, G. A.; Nakatsuji, H.; Caricato, M.; Li, X.; Hratchian, H. P.; Izmaylov, A.F.; Bloino, J.; Zheng, G.; Sonnenberg, J. L.; Hada, M. ; Ehara, M.; Toyota, K.; Fukuda, R.; Hasegawa, J.; Ishida, M.; Nakajima, T.; Honda, Y.; Kitao, O.; Nakai, H.; Vreven, T.; Montgomery, J. A.; Peralta, J.E.; Ogliaro, F.; Bearpark, M.; Heyd, J. J.; Brothers, E.; Kudin, K.N.; Staroverov, V. N.; Kobayashi, R.; Normand, J.; Raghavachari, K.; Rendell, A.; Burant, J. C.; Iyengar, S.S.; Tomasi, J.; Cossi, M.; Rega, N.; Millam, J. M.; Klene, M.; Knox, J. E.; Cross, J. B.; Bakken, V.; Adamo, C.; Jaramillo, J.; Gomperts, R.; Stratmann, R. E.; Yazyev, O.; Austin, A. J.; Cammi, R.; Pomelli, C. ; Ochterski, J. W.; Martin, R. L.; Morokuma, K.; Zakrzewski, V.G.; Voth, G. A.; Salvador, P.; Dannenberg, J.J.; Dapprich, S.; Daniels, A. D. ; Farkas, O.; Foresman, J. B.; Ortiz, J. V.; Cioslowski, J.; Fox, D. J. Gaussian, Inc., Wallingford CT, (**2009**).
6. Becke, A. D. *J. Chem. Phys.* **1993**, 98, 5648.
7. Lee, C.; Yang, W.; Parr, R. G. *Phys. Rev. B* **1988**, 37, 785.